

# A validated CFD Model for Simulation of Cryogenic Fluid Leakage

B. Yerly\*, R. Marcer\*, C. Audiffren\*, M. Rivot\*\* and B. Lequime\*\*  
Corresponding author: richard.marcer@principia.fr

\* Principia, France

\*\* Technip, France

**Abstract:** LNG (Liquefied Natural Gas) accidental cryogenic spillage is one of the major safety concerns of the new Floating LNG facilities. Many critical elements like primary structures, deck and equipment supports shall be properly protected against these hazards, using very costly and constraining passive cryogenic spill protection materials, thus requiring optimization efforts. Stakes of Quantitative Risk Assessment and safety studies performed in FLNG detailed engineering require advanced knowledge and high-fidelity modelling capabilities.

The EOLE 3D CFD model has been developed by Principia to simulate the complex physics of a cryogenic LNG leak. The software has been validated based on mid-scale experiments with liquid nitrogen performed as part of a JIP led by Technip with six other sponsors, at its Cybernetix cryogenic testing facilities in France. Some keys validation results are presented in the paper.

*Keywords:* LNG, thermal transfer, vaporization, boiling curve, EOLE CFD software, validation

## 1 Introduction

A LNG leak, originated for instance from a pipe rupture, involves very complex physical phenomena, more particularly, cryogenic liquid jet fragmentation, vaporization, flashing, rainout, pool formation, spreading, thermal transfer with solid and liquid substrates.

CFD approach is deemed to be the most accurate way to simulate the overall behaviour of the release. In the frame of a Joint Industry Project [1] the 3D CFD software EOLE capabilities, developed by Principia, have been extended to LNG leak simulation [2], [3]. The CFD code is based on an Unsteady Reynolds Averaged Navier-Stokes (URANS) model using coupled Volume of Fluid (VOF) and mixture models, which allows simulation of all dynamic / thermodynamic processes of LNG multi-phases flows, i.e. most of the physics of accidental cryogenic leaks that may occur in Floating LNG topsides or in an onshore LNG plant.

Validation of the code has been carried out as part of the JIP program [1], on results of an extensive mid-scale experimental program which involved more than 120 tests using >150 T of liquid nitrogen; a step-by-step approach has been followed. A specific physical problem was investigated and resolved at each step. Into that frame, the paper presents a sample of validation results:

- Characterization of the boiling curve of a cryogenic fluid in contact with a warm solid substrate and validation on experimental results from the literature.
- Corresponding thermal transfer through the solid substrate, and validation on “thermal conductivity trials”.

- Spillage from an unpressurized liquid tank, pool spreading on a warm solid plate and associated vaporization rate. Validation on “cryogenic pool trials” carried out on a dedicated bench.

## 2 Numerical Model

### 2.1 Required CFD model capabilities for LNG physics

When a leak occurs on equipment containing a cryogenic liquid (pipe rupture for instance), the spillage involves different processes, e.g.: low or high pressure jet spreading in the ambient medium, rainout of the biggest droplets, pool formation on a substrate (solid or liquid), thermal transfer and vaporization of droplets in air and in contact with the warm substrate, pool spreading on the substrate. The required capabilities of the CFD model to simulate such physics are the following:

- Low pressure liquid jet with no or little flashing: the fluid interface model must allow to capture complex processes like instabilities and fragmentation of the interface initiated by the shear stress between liquid and air flows. This “primary break-up” of the jet from which are issued liquid ligaments and droplets is directly computed by a Volume Of Fluid (VOF) model without additional empirical break-up model. The model includes the surface tension force which may be not negligible with respect to inertia especially for the smaller ligaments.
- Two-phase jet: when the release pressure increases, the jet becomes fully fragmented (due to mechanical fragmentation and flashing) and the flow appears as a dispersed droplets phase evolving in a continuous vapour phase. For the smaller droplets which size is “under cell size discretization”, the VOF model is no longer able to represent them in the mesh, so a coupling with an Eulerian “mixture” model for these smaller structures is required. In this model the phases are treated as interpenetrating continua, meaning without interfaces between phases. A volume fraction function for the small droplets is introduced allowing to characterize the mixing of the secondary phase (droplets) into the continuous phase (air, vapour). Then the droplets are represented in the mesh by this function as for the VOF model but contrary to the latter which is based on a specific transport equation for sharp discontinuities (the interfaces), the eulerian “mixture” model is a classical transport equation (including an added term to account for drag and buoyancy of the droplets and relative velocity between phases).
- Several liquids may be present, water and cryogenic liquid (e.g. LNG), meaning co-existence of different kinds of interface (LNG / water or vapour, water / air or vapour).
- Local representation of the fluid characteristics (density, viscosity, thermal transfer) in each cell of the mesh. For a cell containing several fluids, the mean characteristics of the mixture are deduced from the volume fraction of the different fluids.
- Thermal interaction between fluids (LNG/water, LNG/air, water/air). The heat transfer between fluids is computed from the direct resolution of the energy equation considering the local properties of the different fluids and their volume fraction in each cell of the mesh.
- Thermal interaction between fluids and solid which can be simulated from a direct calculation of the thermal fluid/solid coupling or from a flux boundary condition on the fluid/solid interface issued from known data (boiling curve for example).
- Vaporization: the energy equation  $mC_p \frac{dT}{dt} = Q - L\dot{q}$  is locally solved (with  $Q$  the heat flux,  $L$  the latent heat of vaporization and  $\dot{q}$  the vaporization rate). This equation allows considering the cooling down due to the latent heat absorbed in transforming the liquid into gas, during vaporization process. The vaporization term  $\dot{q}$  is also integrated as a source term in the VOF and

mixture equations representing the cryogenic liquid (pure liquid with VOF model or dispersed droplets with mixture model).

- LNG vapour (methane) dispersion in air computed from a convection-diffusion scalar equation. The term  $\dot{q}$  is integrated as a source term in this equation.
- Buoyancy effects (natural convection) computed from density gradients in the fluids: LNG over water (about half density of water), methane in air.

## 2.2 EOLE CFD model

Regarding the physics described above, the numerical model is based on the 3D multi-phase Navier-Stokes system, with a k- $\epsilon$  model for turbulence, and multi-interfaces models of VOF type. As different kinds of interface are involved (LNG / water or vapour, water / air or vapour), a VOF equation is considered for each phase.

Thermodynamic properties (density, viscosity, thermal conductivity and specific heat) are calculated using the volume fractions  $F_1$  (LNG) and  $F_2$  (water). Writing subscripts  $l$  and  $v$  corresponding to liquid and vapour, and  $\phi$  a given thermodynamic property, we have:

$$\phi = F_1\phi_{l\text{ LNG}} + F_2\phi_{l\text{ water}} + (1 - (F_1 + F_2))\phi_v$$

To prevent the two liquid phases, LNG and water, from penetrating into each other (non-miscible fluids), LNG and water interface motions are constrained such as  $F_1 + F_2 = 1$ .

Vaporization / condensation are included as source terms and an additional scalar transport equation is introduced for the vaporized gas concentration.

By assuming that phase change occurs at a quasi-thermo-equilibrium state and at constant pressure, and assuming that the mass transfer rate  $\dot{q}$  is mainly led by the temperature difference  $T_c - T_{sat}$ , the source terms are written as follows:

- Vaporization of liquid:  $\dot{q} = r_l F_l \rho_l \left( \frac{T_c - T_{sat}}{T_{sat}} \right)$  with  $T_c \geq T_{sat}$
- Condensation of gas:  $\dot{q} = r_v F_v \rho_v \left( \frac{T_c - T_{sat}}{T_{sat}} \right)$  with  $T_c < T_{sat}$

with  $T_c$  the local temperature in a given cell,  $T_{sat}$  the saturation temperature,  $F_l$  and  $F_v$  the local volumetric fractions,  $r_l$  and  $r_v$  constant parameters.

A mixture model is used to simulate the small droplets dispersed phase which cannot be represented by the VOF model. The code is so able to switch from VOF to mixture depending of the size of the liquid ligaments and droplets. This VOF / mixture models coupling is described in [2]. Vaporization / condensation source terms have similar formulations as for the VOF model described above.

## 3 Results

### 3.1 Boiling curve simulations

These simulations consist in modelling a cryogenic liquid layer heated at the bottom wall. The objective is to identify the different boiling stages and associated heat flux at the wall. The wall temperature and vaporization drive the heat transfer from the bottom surface to the liquid, resulting in different boiling regime, film, transition or nucleate boiling.

The calculation domain size is the same as the one described in [4], 4.59 mm width and 13.76 mm height, with a discretization of 64 x 192 cells respectively.

The fluid block is initially filled with 10 mm height Liquid Nitrogen (LN2) at rest and at 77K.

Liquid nitrogen properties are constant:

$$\rho = 810 \text{ kg.m}^{-3}, \mu = 1.56 \times 10^{-4} \text{ Pa.s}, C_p = 2112 \text{ J.kg}^{-1} \cdot \text{K}^{-1}, \lambda = 1.38 \times 10^{-1} \text{ Wm}^{-1} \cdot \text{K}^{-1}$$

Regarding the thermal behaviour, adiabatic (zero thermal flux) conditions are used at the lateral and top boundaries. Different wall temperatures are imposed at the bottom boundary to obtain different boiling regimes.

The boundary conditions are summarized on Figure 1.

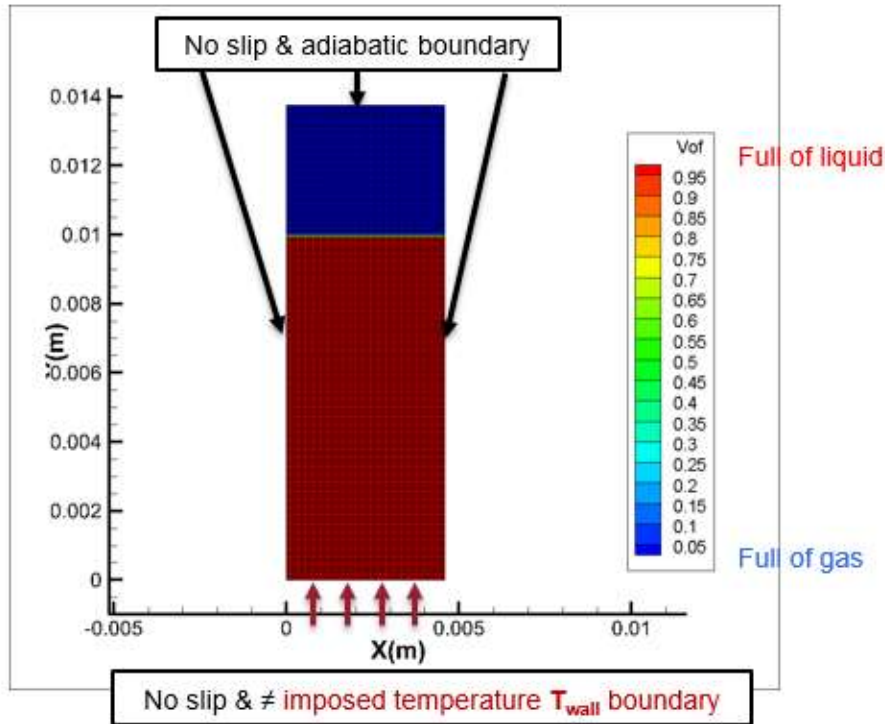


Figure 1: Boundary conditions for the boiling curve model

The fluid is progressively warmed up at the bottom wall. Due to vaporization process, a very thin film of vapour is created and thickens with the heating supply from the wall (Figure 2). Then as the wall temperature increases the film becomes unstable and breaks into bubbles separating from the solid surface. The vapour film is disrupted and part of the surface is exposed to the liquid, leading to the transition regime of boiling.

The motion of the bubbles under buoyancy effect enhances the motion of the liquid, increasing turbulence and mixing near the wall, and then convective heat transfer. The bubbles escape as jets or columns and sometimes merge into bigger slugs of vapour.

On Figure 3 the boiling curve obtained with the model (solid line) is compared with the dashed black line corresponding to an average of collected boiling curves from literature [5].

The boiling curve obtained with EOLE is very close to the experimental one and especially highlights the change in boiling regimes between nucleate and transition, and between transition and film boiling corresponding to line inflection slopes for a temperature difference between 100-110K.

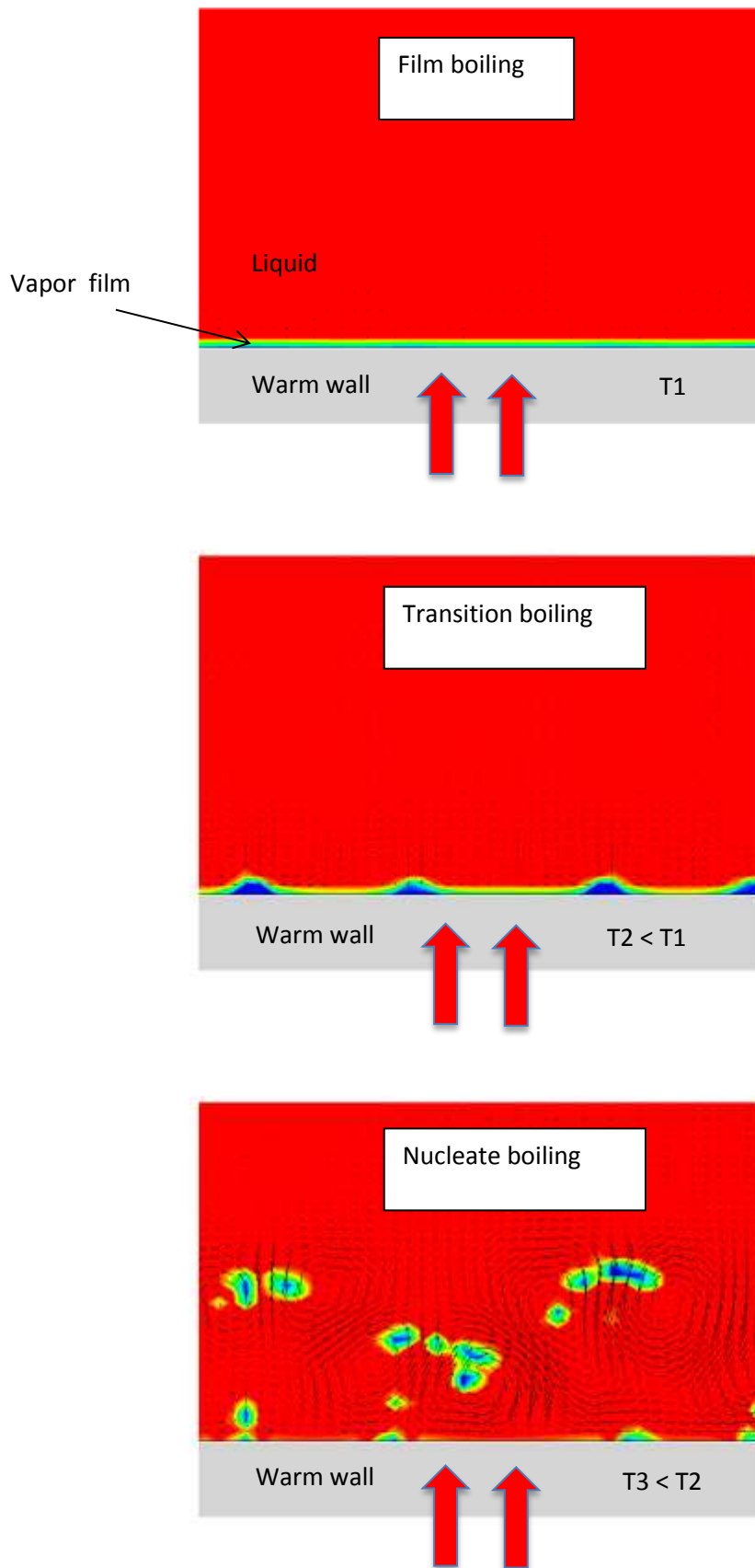


Figure 2: Different regimes of the LN2 boiling dependig of  $\Delta T = T_{\text{wall}} - T_{\text{fluid}}$

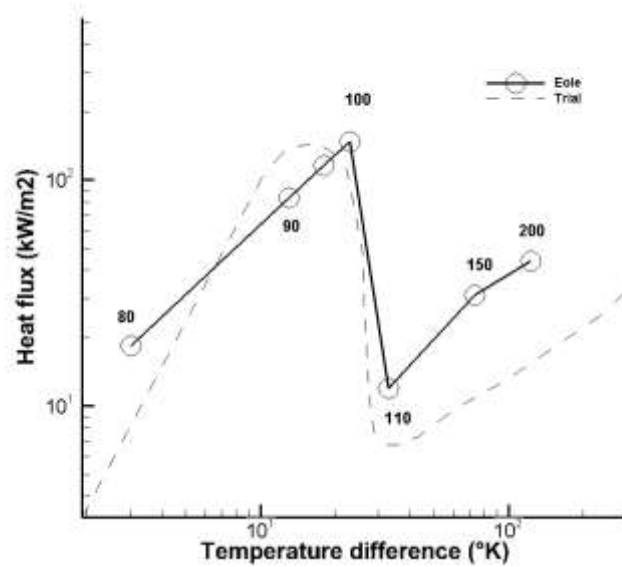


Figure 3: Boiling curves from EOLE simulations versus experimental curve from literature [5]

### 3.2 Thermal conductivity simulations

Thermal conductivity simulations aim at qualifying the code on fluid / solid thermal coupling and especially on the cooling down of the solid in contact with the cold liquid.

Results are compared with experimental data from thermal conductivity trials carried out in Technip cryogenic facilities. The test bench is a square bottom shape basin of 20 cm edge length filled with liquid nitrogen.

The calculation domain is a 2D model of the test bench. The mesh includes two blocks, a solid block of 1 cm height modelling the carbon steel plate and a fluid block modelling a column of 15 cm height liquid nitrogen at rest. Initial temperatures are 77K for the fluid and 293°K for the solid.

Liquid nitrogen properties are the same as given in §3.1 for boiling simulation.

For carbon steel properties,  $C_p$  and  $\lambda$  are variable versus temperature and  $\rho = 7850 \text{ kg.m}^{-3}$ .

A temperature of 77 K is imposed at the fluid top and lateral boundaries assuming that the gas phase, mainly composed of nitrogen vapour, has a temperature close to the liquid nitrogen saturation temperature. Adiabatic (zero thermal flux) conditions are used for the solid boundaries except for the fluid/solid interface as an insulating foam frame has been used in the experimental test bench to minimize lateral and backface heat transfer.

The boundary conditions are summarized on Figure 4:

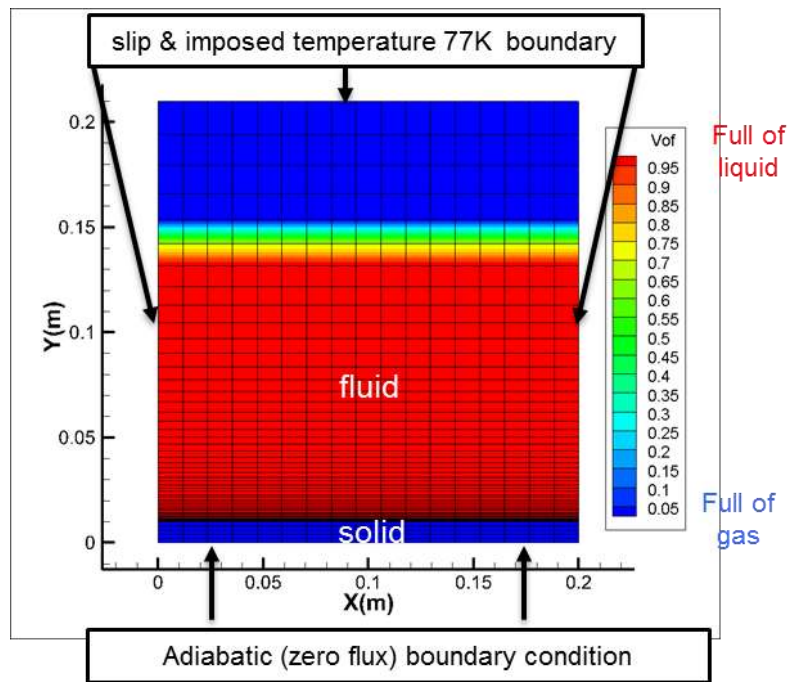


Figure 4: Boundary conditions for the thermal conductivity model

A probe located under the plate allows following the temperature time evolution due to conduction through the plate in contact with the liquid. It is compared with the experimental temperature measured by a thermocouple located at the same position on the carbon steel plate backface.

In these thermal conductivity simulations heat flux at the liquid / solid interface is imposed following the profile based on an experimental nitrogen boiling curve. The imposed heat flux is a function of the local temperature difference at the interface between the plate and the fluid.

On Figure 5 solid line corresponds to simulation and dotted/dashed lines to experiments for different reproducibility trials carried out in the same conditions. The numerical model is able to reproduce the right time of arrival of the curve inflection points, the first around 150K (between 150s – 200s) and the second highlighted around 100K. These inflection points are associated physically to a change in the boiling process. The first one corresponds to the change from film boiling to transition regime occurring at a critical delta ( $T_{wall} - T_{sat}$ ) of temperature of about 30-60K on the literature boiling curves (Leidenfrost point), and the second corresponds to the change from transition to nucleate regime occurring at a critical delta of temperature of about 10K on the literature boiling curves (Critical Heat Flux point).

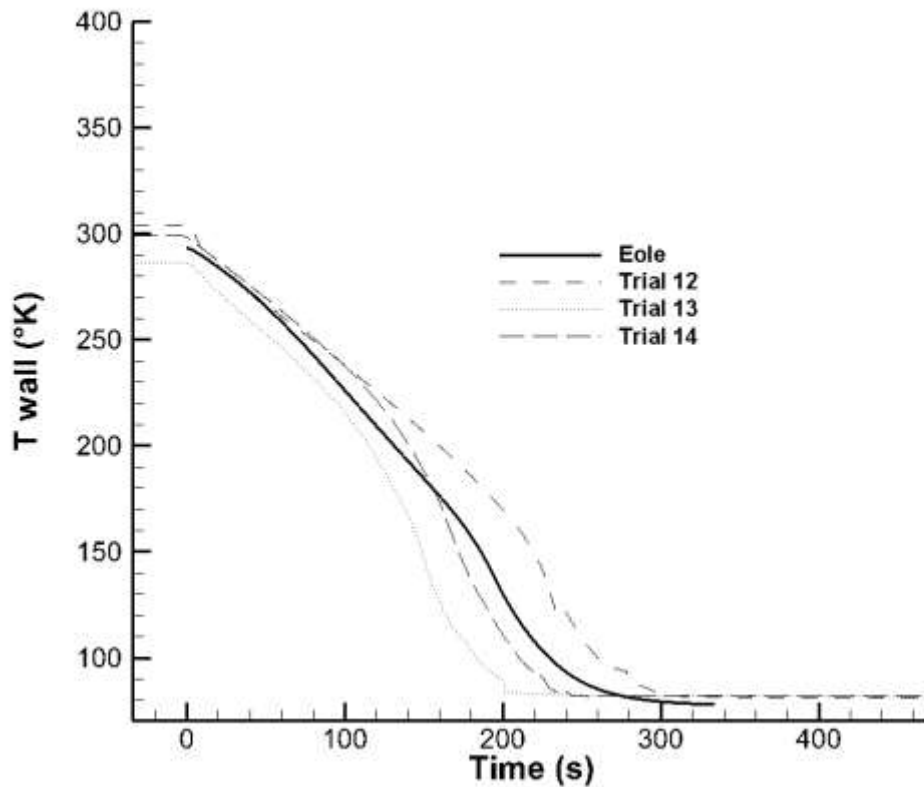


Figure 5: Comparison of time evolution temperature profiles on a probe located under the plate

### 3.2 Running cryogenic pool simulations

These simulations aim at qualifying the code on two important physical phenomena in the spillage problem, the pool spreading on a warm solid plate and the associated vaporization rate.

The calculation domain is a model of the test bench [3], [6] which is composed of a carbon steel plate (4m length and 1cm thickness) with a slope of 3%. A spillage tank is located above the “high point”, from which the liquid nitrogen is released by mean of a 50 mm nozzle placed at 5 cm above the plate (Figure 6). A recovery tank at the end of the plate allows collecting the liquid which has not been vaporized on contact with the warm plate and the ambient air.

Considering half of the geometry (symmetry condition according to a longitudinal plane), the mesh size of the system is 200 000 cells.

Two different initial volumes in the spillage tank are investigated, 500 L and 250 L.

Fluid and solid (plate in carbon steel) properties are the same as for the thermal conductivity case presented above.

Initial temperature of liquid is 77K whereas air and solid are at ambient temperature 283K.



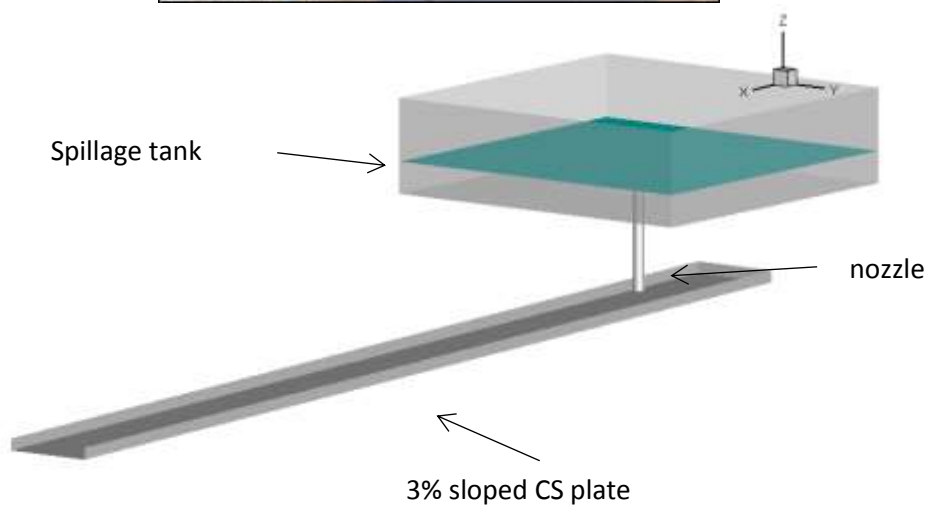
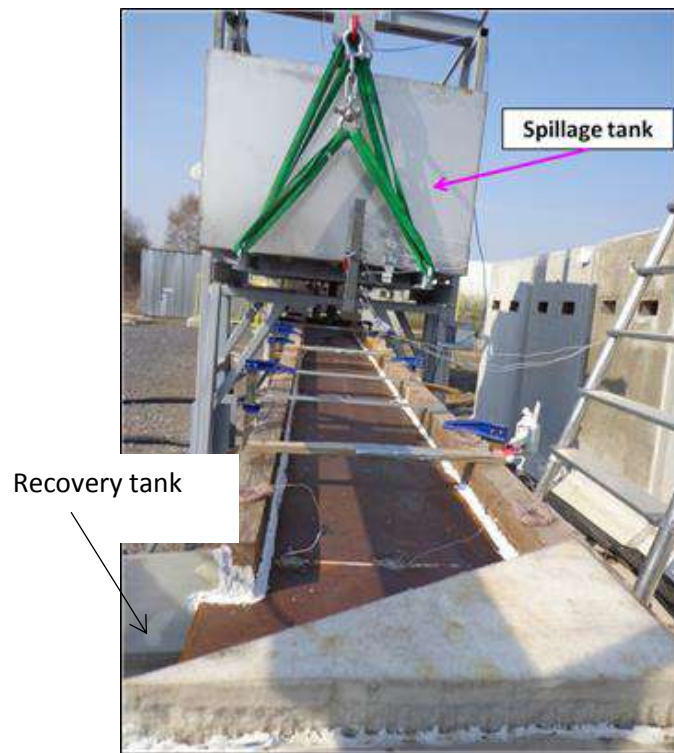


Figure 6: Test-bench (top) and numerical model (bottom)

The initial pool velocity is measured during the first seconds of the release ( $< 4s$ ) from the instant the liquid nitrogen impacts the plate (Figure 7) until the pool front reaches the end of the plate and enters in the recovery tank. This short phase corresponds to the highest dynamic phase of the flow during all the spillage process. The time step was chosen accordingly, small enough (here 1ms) to accurately represent the pool propagation.

A mean velocity value of the pool front has been extracted from a monitoring of the distance travelled by the front pool between different instants (Figure 8). A value of 1.5m/s is highlighted which is very similar to the one brought out in the experiments from visualizations obtained with a thermal camera.

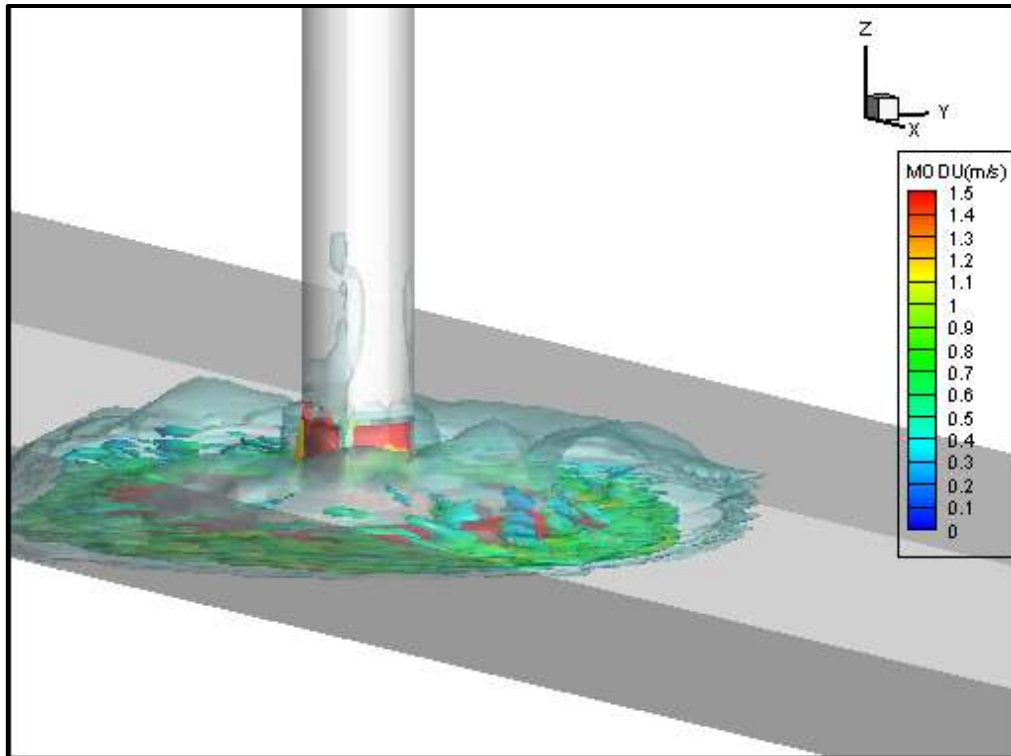


Figure 7: Formation of the pool on the plate just after the jet impact. Liquid interface coloured with the velocity modulus and vaporized gas in light blue

As for the experiments, a liquid nitrogen vaporization rate is computed by analysing the difference between the spillage tank liquid volume ( $V_s$ ) at the initial time and the recovery tank liquid volume ( $V_r$ ) at the end of the spillage process. This volume difference  $V_s - V_r$  corresponds to the amount of liquid nitrogen that has been vaporized during the overall process.

In the simulation, the time evolution of the spillage and recovery tank volumes is issued from the flow rate integration, respectively:

- At the nozzle outlet where it is assumed that no vaporization has still occurred (released volume).
- On a section at the end of the plate (recovered volume) which includes the vaporization processes of the liquid pool with the plate and with the surrounding air.

The corresponding curves compared with the experiments for different initial spillage tank liquid volumes show the ability of the code to reproduce the combined and complex dynamical release and thermodynamic vaporization rate processes (Figure 9 and Figure 10).

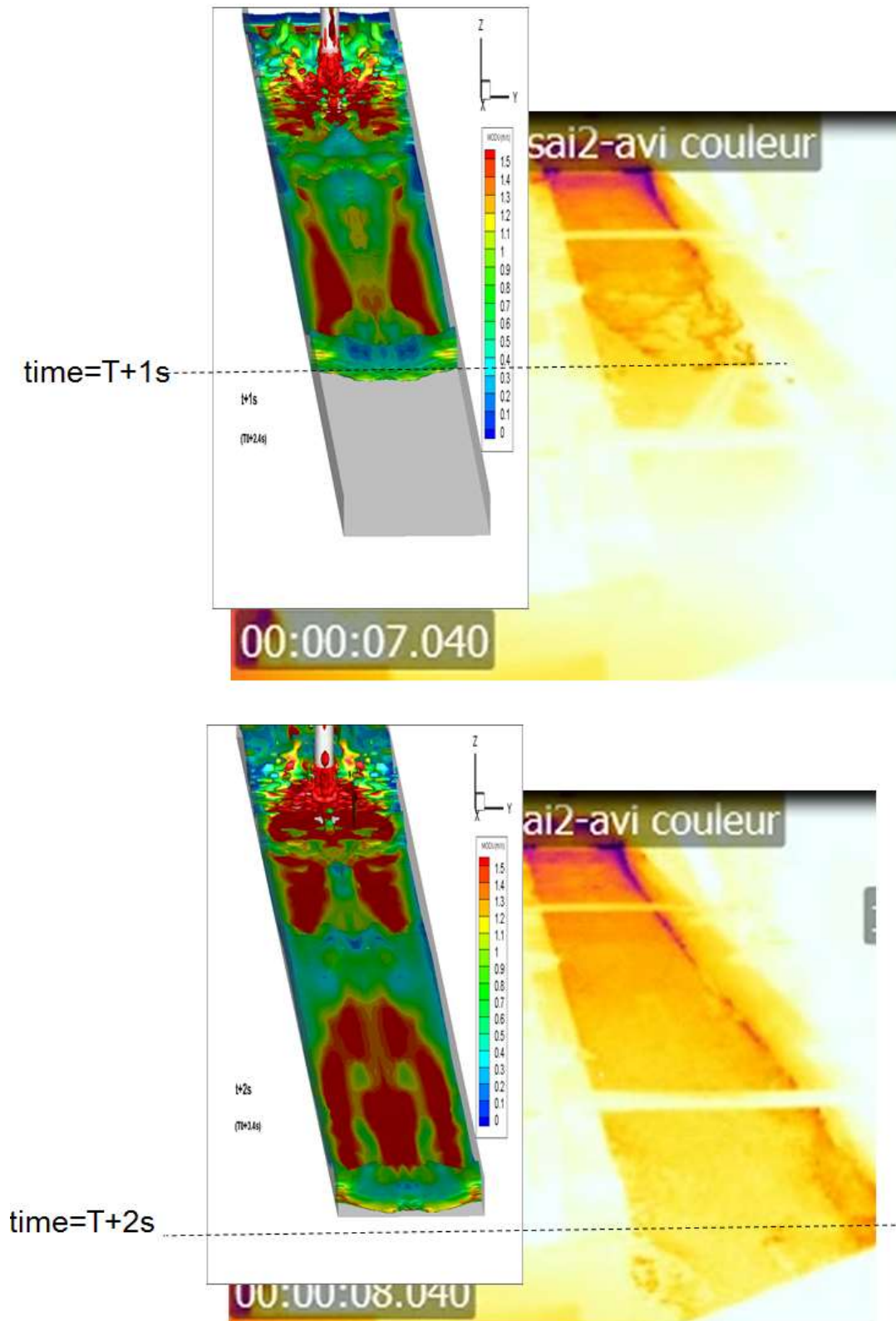


Figure 8: Comparison simulation / experiments (thermal camera) of the pool front interface propagation at two instants (one second gap). Liquid interface colored by the velocity modulus.

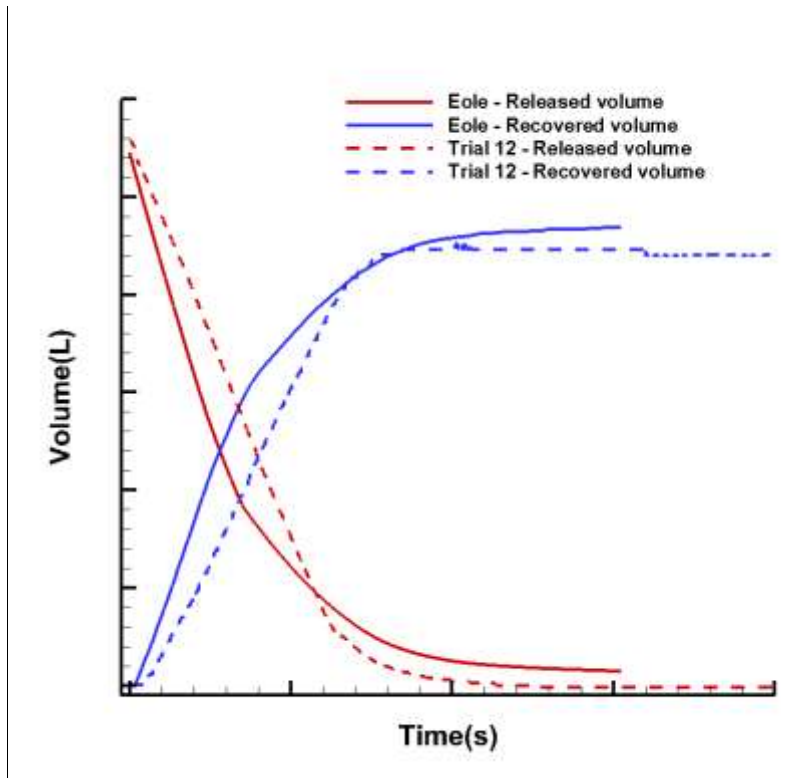


Figure 9: Spillage volume ( $V_s$ ) and recovered volume ( $V_r$ ) time evolution – 500 L

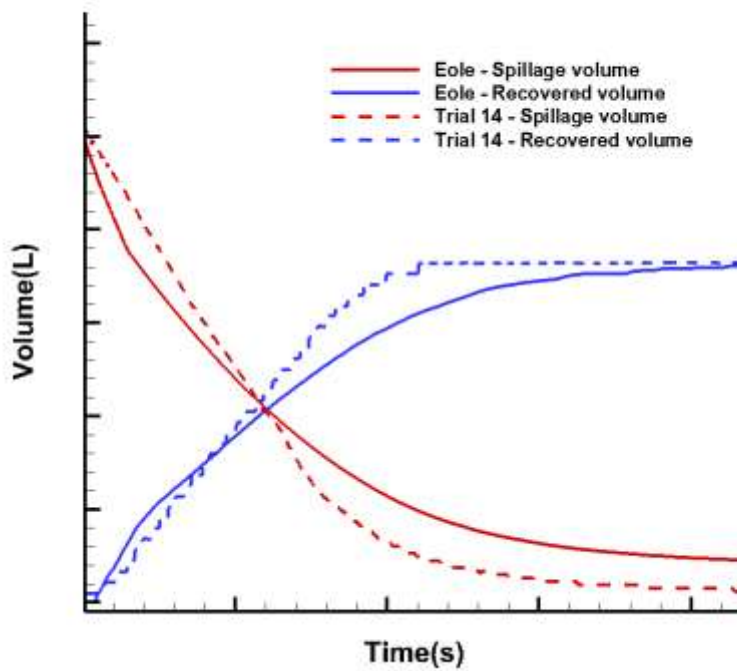


Figure 10: Released and recovered time evolution volumes – 250 L

Figure 11 below displays vaporization rates in % ( $1 - V_r/V_s$ ) for trials and simulations, and for two different initial volumes in the spillage tank, for which several trials have been carried out.

The numerical model gives satisfactory results and is especially able to bring out the decrease of the average vaporization rate when the LN2 inventory released increases, the temperature of the plate and the surrounding gas becoming lower (due to a longer release duration).

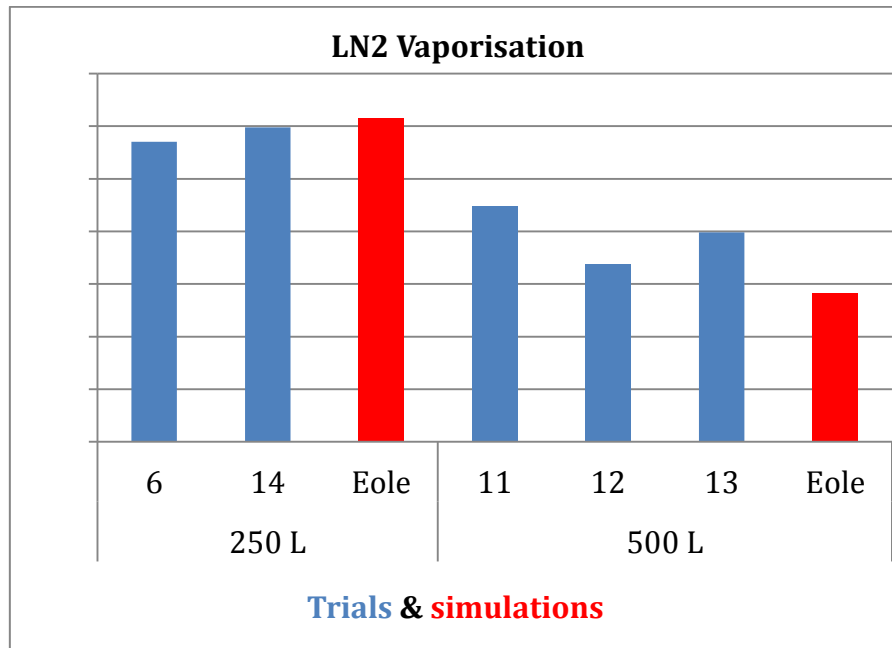


Figure 11: Vaporization rate – Comparison trials (blue) versus simulations (red)

## 4 Conclusion

As part of the qualification of the EOLE CFD model in the JIP project, complex physical processes encountered in cryogenic fluid leak and spillage processes have been validated:

- Boiling curve for cryogenic fluid (nitrogen).
- Heat transfer with steel plate.
- Spillage of liquid onto a plate, liquid pool velocity and vaporization.

A Verification & Validation (V&V) methodology has also been implemented to reinforce the validity domain and accuracy level of the CFD code which is currently used for the simulation of accidental cryogenic releases performed as part of the quantified Cryogenic Spill Risk Analyses of industrial facilities projects.

## References

- [1] Joint Industry Project – FLNG Cryogenic Spillage Protection WP3. Qualification of EOLE for cryogenic spillage applications.
- [2] R. Marcer, B. Yerly, L. Pomié, B. Lequime, M. Rivot, E. de Carvalho, F. Baillou, CFD Simulation of LNG Spillage, ECFD VI, Barcelona, July 2014. <http://dx.doi.org/10.13140/RG.2.1.4624.1361>
- [3] M. Rivot, B. Lequime, E. de Carvalho, M.G. Molina-Borregales, N. Noel, R. Marcer, B. Yerly, C. Audiffren, R. Legent, V. Tomsa, Experimental Tests and Qualification of a CFD Simulation Tool for Cryogenic Release Modelling through the JIP “FLNG Cryogenic Spillage Protection”, GPAe Annual Conference, Budapest, September 13-15, 2017.
- [4] Y. Liu, T. Olewski, L. Vechot, X. Gao, S. Mannan, 14<sup>th</sup> Annual Symposium, Mary Kay O’Connor Process Safety Center, Texas A&M University, October 25-27, 2011.
- [5] R.F. Barron, Cryogenic heat transfer; CRC Press, 1999.
- [6] B. Yerly, R. Marcer, C. Audiffren, M. Rivot, B. Lequime, R. Legent, Experimental Qualification of a CFD model for simulation on LNG Spillage on Solid Structures. MULTIPHASE 2017, 17<sup>th</sup> International Workshop on trends in numerical and physical modeling for industrial multiphase flows, ENS Paris-Saclay, October 16-18, 2017.